

# Detection of Choroidal Neovascularization through Parametric Modeling of the Intensity Variation in Fluorescein Angiograms

Anitha Gunasekaran<sup>1</sup> and M. Mohamed Ismail<sup>2</sup>

*Department of EIE<sup>1</sup>, Department of ECE<sup>2</sup>*

*B. S. Abdur Rahman Crescent Institute of science and Technology, Chennai, India*

*anidhag@crescent.education*

[mmismail@crescent.education](mailto:mmismail@crescent.education)

**Abstract:** Choroidal Neovascularization (CNV) is a devastating sequela resulting from a wide range of disorders that affect the Retinal Pigment Epithelium (RPE)-Bruch's membrane-choriocapillaris complex. That is popularly known as Age Regulated Degeneration (AMD), which is the leading cause of permanent serious loss of vision among senior citizens in the developed parts of the world. A mathematical model implemented in this work is used to detect the stages of CNV using artificial intelligence technique. This model is developed based on the intensity variation caused by the size of lesions in the FA (fluorescein angiography) sequence with respect to time. A collection of features is calculated from the mathematical model, and a feature vector is constructed using those features. These feature vectors are used to categorize the severity of the disease through a classifier. The mathematical model of lesions in CNV is used to find out the pattern that CNV follows which enhances the pattern recognition capabilities of the classifier. Defining CNV lesions is typically a time-consuming and tiresome task. Therefore, this proposed method of developing a mathematical model of the intensity variation in the FAs will help to identify CNV efficiently. Irrespective of the machine learning classifiers, this model provides good accuracy, sensitivity, and specificity and F1 score.

**Keywords:** Fluorescein Angiography, Choroidal Neovascularization, Machine learning, Parametric Modeling, Age Regulated Degeneration, Deep learning

## 1. INTRODUCTION

Choroidal neovascularization (CNV) is a medical condition involving the growth of new blood vessels originating from the choroid (the layer of blood vessels between the retina and the sclera) into the subretinal space [1]. This abnormal growth can lead to significant vision impairment and is commonly associated with several eye diseases. Diagnosis typically involves a combination of the following: fundus examination, which is used to visually inspect the back of the eye; optical coherence tomography (OCT), an imaging technology that provides cross-sectional views of the retina; fluorescein angiography, which uses a fluorescent dye to visualize blood flow in the retina and choroid; and indocyanine green angiography, another dye test useful for detecting choroid blood vessels. Fluorescein Angiography (FA) provides several advantages. It offers detailed images of the blood vessels in the retina and choroid, making it particularly useful for detecting and evaluating blood vessel abnormalities, leakage, and neovascularization. Additionally, FA is excellent at identifying areas of active leakage, which is crucial for diagnosing conditions like CNV and diabetic retinopathy.

The fluorescein angiography procedure involves several steps to effectively visualize and assess the blood flow in the retina and choroid. The patient is informed about the procedure, its purpose, and potential risks. Consent is obtained. Eye drops are administered to dilate the pupils, allowing better visualization of the retina. The patient is asked about any allergies, particularly to fluorescein dye or iodine, to minimize the risk of adverse reactions. A small amount of fluorescein dye (usually 5 mL) is injected into a vein in the patient's arm or hand. As the dye

travels through the bloodstream to the eye, a special camera equipped with filters takes a series of rapid photographs of the retina and choroid.

The images obtained at the early, mid, and late phases of fluorescein angiography provide distinct and valuable information about retinal and choroidal blood flow and potential abnormalities. Early phase usually begins within 10-15 seconds after the injection. The retinal arteries and choroidal vessels begin to fill with dye, appearing bright and well-defined. The choroidal flush occurs first, with the dye rapidly filling the choroidal vessels and then the retinal arteries. This phase helps assess the integrity and perfusion of the retinal arteries. Mid phase is approximately 30 seconds to 2 minutes after injection. The dye spreads into the retinal veins after filling the retinal arteries. Retinal veins start to fill, and there is usually a complete filling of the retinal vascular system. This phase helps visualize the transition of dye from arteries to veins, highlighting any blockages, abnormal vessel patterns, or areas of leakage. Late phase around 5-10 minutes after injection. The dye gradually diminishes in the retinal vessels and is primarily visible in the extracellular space. This phase is crucial for identifying areas of persistent leakage or staining, indicating the presence of neovascularization, retinal edema, or other pathologies. Abnormalities like microaneurysms, neovascular membranes, or damaged blood-retinal barriers can be identified as hyperfluorescent spots or areas. These phases collectively help in diagnosing and evaluating conditions such as diabetic retinopathy, age-related macular degeneration, choroidal neovascularization, and other vascular abnormalities. By comparing the images across these phases, ophthalmologists can determine the extent and nature of the vascular abnormalities and plan appropriate treatment strategies.

Analyzing fluorescein angiography images using ML techniques can significantly enhance the accuracy and efficiency of identifying retinal abnormalities. In this work, a mathematical model is developed by studying intensity variation in early, mid and late phases of FA. The features obtained from the mathematical modeling are given as inputs to the ML classifiers. These features derived from the model improve the classification capability of the ML classifiers.

Fundus FA is a standard diagnostic and screening technique for several retinal diseases. FA images are evaluated qualitatively by trained observers and are thus susceptible to inter- and intra-observer variability. Unlike OCT, FA is a sequence consisting of a set of frames in which the intensity of each frame is varied with respect to time. Hence, studying the intensity variation in each frame of the FA sequence will help in the measurement of the severity of CNV. In each FA sequence, the intensity of the retinal images varies with the concentration of fluorescein dye. In a FA, approximately two tablespoons of sofa dye (not related to iodine, which contains x-ray dyes) are injected into the vein in the patient's arm. Lots of consecutive images are captured as this dye circulates through the eye. In this FA image, the dye appears white as it fills the vessels. Since the formation of CNV lesions is clearly depicted, identifying the different stages of CNV, namely classic and occult, through their fluorescence patterns becomes easier.

In 1989, Chamberlin, J. A. et al. [2] developed a set of techniques for analyzing FAs. These techniques are used to find out the location and extent of CNV. Berger JW and Yoken J proposed a computer-assisted method for the quantitation of CNV [3]. They examined 30 images in 5 patients, and two metrics were calculated: First, the lesion area. Second, integrated lesion intensity. They have concluded that this quantitation of CNV may be useful for the support of clinical trials and preclinical studies. Sayed M. Shah et al [4] reported a technique for detecting changes in lesions area and intensity varying with respect to time. After dye injection, the values for each frame are plotted against time to produce curves, and each region under the curve (AUC) is measured. Compared to previous approaches, this method offers a benefit in evaluating treatment outcomes that may boost the reliability of FA as a measure of outcome in clinical trials.

Harihar Narasimha Iyer et al. [5] suggested a method for identifying and classifying the changes in FA longitudinal time series automatically. To classify the different stages of the disease, the variations in the CNV-affected areas are examined. Automatic segmentation is done

to separate features such as the fovea, optic disc, vasculature, and vessel branching. The region of interest (ROI) is cropped, and changes in that region are measured. The Bayesian Classifier categorizes the variations into different stages of CNV with an accuracy of 83%. E. Brankin et al. [6] investigated the use of gradient vector flow active contours to identify CNV from fundus FA in exudative AMD. However, a fully automated identification of CNV is needed to lessen the inter- and intra-observer variability and also to decrease the effort involved and the time spent. In 2011, Ahmed S. Fahmy et al. [7] developed a method to automatically segment CNV lesions by analyzing variations in the temporal intensity of FA sequences. This method identified and classified CNV into three stages: Occult, Classic and background. In 2013, Walid M. Abdelmoula et al. [8] also presented the same kind of work for the segmentation of CNV. The preliminary tests were performed on 21 Wet-AMD patients' data, and the results show that the segmentation ability of the system is almost as close as manual segmentation.

Lin, K. S., et al. [9] proposed a scheme for producing a CNV lesion severity map and assessing the different stages of CNV in the FA sequence. A feature vector has been developed that consists of intensity values, intensity changes, and the area of fluorescence leakage. These factors are entered into an SVM classification engine that gives a recognition rate of 85.7%. In 2010, Khurana R et al [11] examined the OCT and FA images of 56 patients with neovascular AMD. They came to know that, compared to FA, OCT often tends to detect anomalies. Chhablani, J et al [10] also compared two imaging modalities for the detection of CNV. They have examined FA and OCT images and reported that the specificity and sensitivity obtained from FA images are 80.4% and 47%, respectively, and for OCT, they are 86.9% & 58.8%. The features collected from the FAs are given to machine learning (ML) classifiers, which are effectively used for the categorization of CNV. Each type of ML technique has its own advantages and disadvantages. By comparing the performance of various ML algorithms, one can identify the best ML that is suitable for its dataset. Each classifier fits each data set in a different manner. Therefore, the selection of an optimal classifier is crucial to achieving peak performance and accuracy.

Muthu Rama Krishnan et al [12] proposed a technique to find AMD, which is characterized by neovascular vessels, drusen, and dead cells in the retina. Features such as pattern occurrence and linear configuration coefficients are measured from fundus images and applied to ML classifiers such as Naive Bayes (NB), Support Vector Machine (SVM), Decision Tree (DT), Probabilistic Neural Network, and K-Nearest Neighbor (*k*NN) to categorize healthy and AMD types. The test was carried out on the DTARE dataset for 22 features, with a classification accuracy of 97.78%. KedarPotdar and RishabKinnerkar [13] examined the performance of different classifiers on the prediction of breast cancer. They have tested *k*NN, Artificial Neural Networks (ANN), and NB classifiers for their study. ANN outperforms the other two classifiers with an accuracy of 97.4 %. NilimaKarankar et al. did a comparative study on NB, *k*NN, SVM, DT, and Gaussian Mixture Model classifiers for the prediction and prevention of cardiac arrest [14].

Nabian M et al [15] examined the classifiers *k*NN, DT, SVM, Logistic regression, NB and Random Forest to identify different real-time human actions like standing, walking, running, and cycling. It has been shown from the tests that Random Forest's performance is better than the other classifiers, with more than 99% accuracy. They also analyzed how Principal Component Analysis (PCA) affects the performance of different classifiers. Amr E. Mohamed [16] studied the classifiers Decision Tree, *k*NN, ANN, and SVM and assessed the performance of these classifiers based on sensitivity and specificity. The analysis has shown that there is no particular test that can provide information about the classifier's performance and that there is no other classifier that can satisfy all of the criteria. Jaspreet Singh et al [17] compared the performance of four classifiers, J48, OneR, BFTree, and Naive Bayes on datasets for sentiment analysis. They discussed and compared the efficiencies of these four classification techniques. Naive Bayes is found to be the

best learning classifier, while OneR is found to be more effective in producing accuracy. Dionisios N. Sotiropoulos et al [18] tackled the issue of pattern classification in sentiment analysis by using SVM. They evaluated the performance of the SVM against other classifiers using a benchmark dataset from the Greek banking sector. SVM produced the best results in terms of precision and time of execution. Poonam Sonar et al [19] proposed an enhanced hybrid kNN-SVM classifier and compared its results with NB, Logistic Regression, Random Forest, Discriminant analysis, kNN, and SVM. A comparative study was conducted using the repositories of normal mammograms from the Mammographic Image Analysis Society (MIAS) and the Digital Database for Screening Mammography (DDSM), as well as brain Magnetic Resonance Imaging (MRI) repositories.

Deep learning (DL), a subset of artificial intelligence, has been extensively utilized in medical imaging and the computer-aided diagnosis of retinal diseases. DL automates feature extraction, whereas ML often requires manual feature engineering. It is highly effective at processing large and complex datasets. DL models, particularly deep neural networks, tend to achieve higher performance in terms of accuracy and efficiency on tasks such as image and speech recognition, natural language processing, and more. DL allows for end-to-end learning, where a model learns directly from raw inputs to final outputs without needing intermediate steps. These advantages make DL a powerful and flexible tool, capable of addressing challenges and achieving results that traditional ML techniques might struggle with.



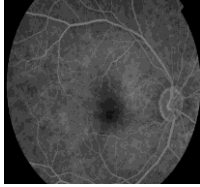
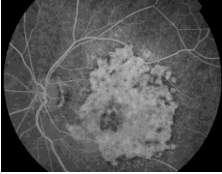
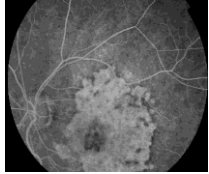
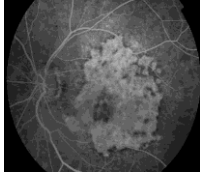
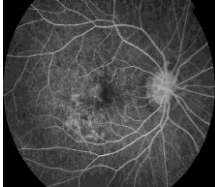
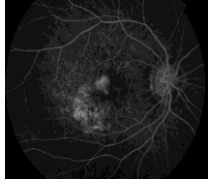
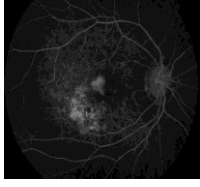
Jose N Galveia et al [20] reviewed the state-of-the-art applications of Convolutional Neural Networks (CNN) in diagnosing common eye diseases. Kai Jin et al [21] developed a multimodal deep learning model with feature-level fusion to identify neovascularization activity in age-related macular degeneration. Jie Wang et al[22] utilized deep learning techniques to diagnose and segment CNV in OCT angiography using a large real-world dataset. These researchers used OCT images and deep learning techniques to detect CNV. However, it is uncommon to find studies that use FA images combined with deep learning techniques for detecting CNV.

In this work, the FA mages are used to detect CNV by using the ML and DL techniques. This work begins with parametric modeling of the temporal variation of the lesions and background intensities. The method is based on the discrepancy in the time-intensity signals between the diseased and normal. The values of the model parameters are used to evaluate the change in the activity of the disease. Therefore, to attain optimum efficiency in these retinal disease prognoses, a comparative study of classifiers is important since a particular classifier may or may not function well for such datasets. In this work, the following classifiers are used to categorize the different stages of CNV: NN, SVM, DT, kNN, Ensemble, and NB classifiers. These classifiers are put to a test based on the time taken to train with the data and how accurate the classification is. The results of the ML classifiers have been compared with those of a deep neural network (DNN) classifier.

## **2. IMAGE ACQUISITION**

An FA sequence has a set of images in which the intensity of pixels varies with respect to time. A collection of 50 FA images of CNV-affected persons was carried out, of which 26 are of classic type and 24 are of occult type. The FA sequences used in this work have been collected from Vasan Eye Hospitals, Chennai, India. A sample of images obtained at the early, mid, and late phases of FA are given in Table 1.

TABLE 1. INITIAL, MIDDLE AND LATE-PHASE ANGIOGRAMS OF NORMAL, CLASSIC AND OCCULT CATEGORIES

Category	Initial phase	Middle phase	Late phase
Normal			
Classic			
Occult			

Every frame of fluorescein angiography is reviewed to get the correct information. The frames that do not cover the complete lesion are discarded. The frames with appropriate exposure are selected through histogram analysis. Figure.1 illustrates how the frames are selected based on analysis of histogram.

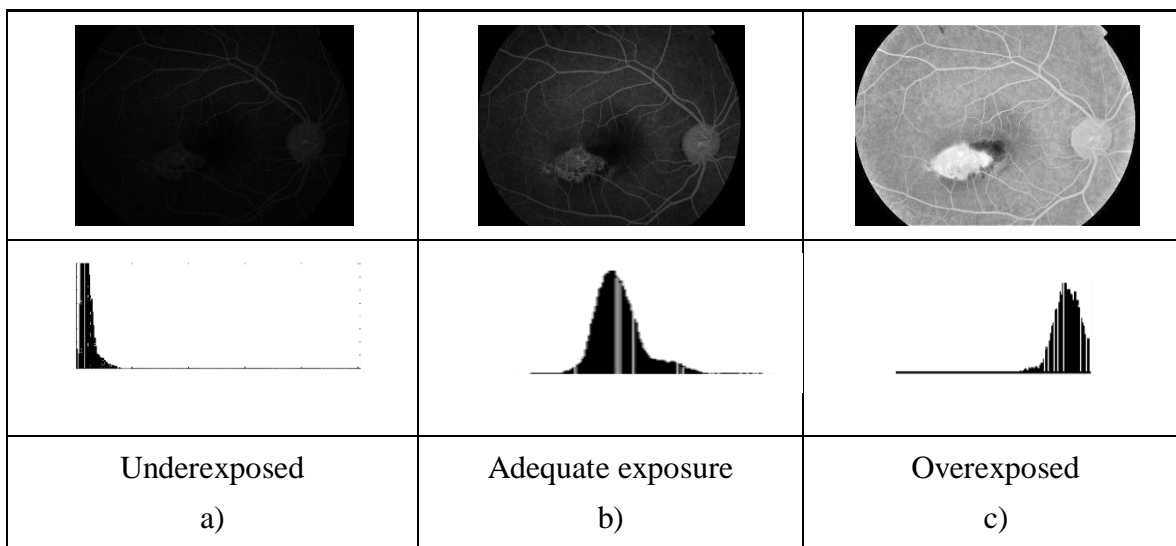


Figure 1: Selection of frames: a) rejected b) selected c) rejected

### 3. PREPROCESSING

Before going to obtain the parametric model, preprocessing operations such as green

channel enhancement, contrast enhancement and cropping region of interest (ROI) have been performed on the fundus images to obtain some valuable information from the fundus images. The CNV-affected areas have a higher intensity compared to other areas in the retina. The CNV-affected region and the normal region are cropped from the images of each FA set and some samples are tabulated. To lessen the computation time and to avoid processing unnecessary data, all the operations are constrained to an ROI of size [519 507], which is shown in the Figure. 2. Then the mean intensity values are calculated from the region consists of lesions and from the normal region. The intensity values computed for both regions of each frame in an FA sequence is shown in Table.2.

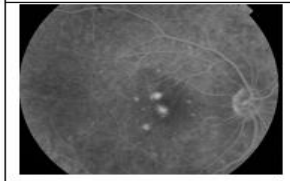
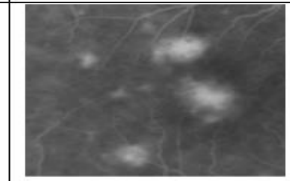
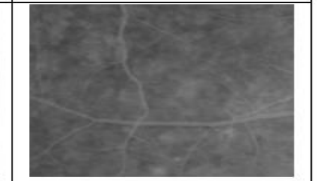
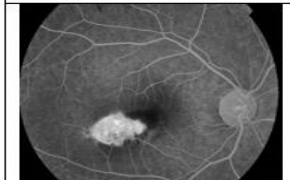
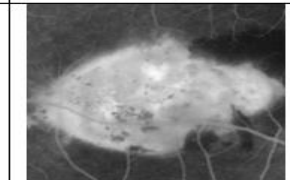
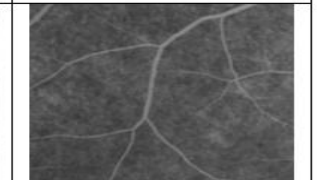
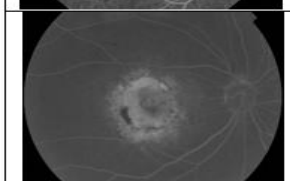


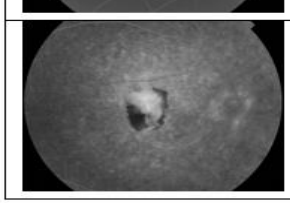
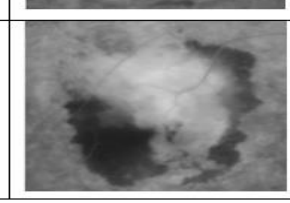
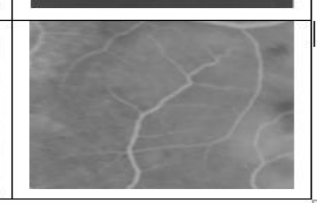
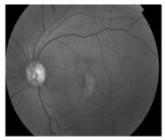
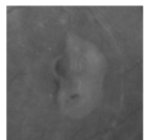
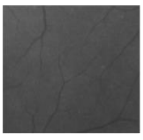
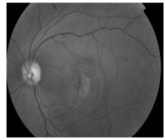
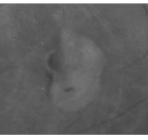
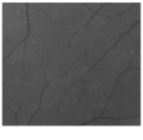
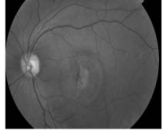


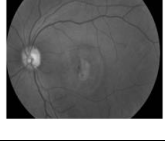


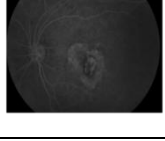


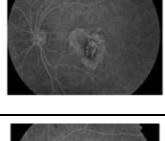
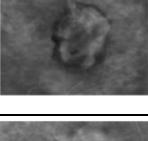
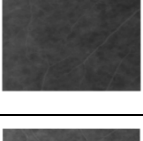
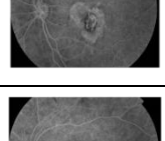
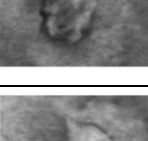
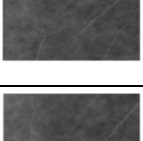
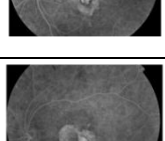
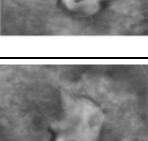
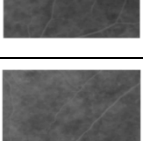
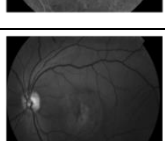
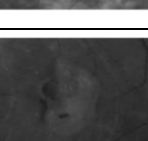
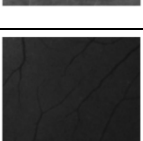



Original Image	Cropped image of affected region	Cropped image of normal region
		
		
		
		

Figure.2. Cropped Images from the FA Images

TABLE 2. MEAN INTENSITY VALUES OF NORMAL AND CNV AFFECTED REGIONS

Frame	Original Image	Cropped Region of affected region	Cropped Region of normal region	Mean Intensity values of affected Region	Mean Intensity values of normal Region
1.				92.60	77.72
2.				92.98	82.19
3.				56.79	43.23
4.				58.43	44.19
5.				58.32	37.21
6.				85.32	62.69
7.				103.52	78.94
8.				125.04	78.32
9.				109.48	89.03
10.				55.07	35.85

## 4 PARAMETRIC MODELING OF TEMPORAL INTENSITY VARIATION

The intensity changes in the FA of normal humans are found to be approximately constant. If a graph is drawn for an FA (affected by CNV) between mean intensity values and frequency of intensity values, it would have a bell-shaped structure as the intensity/pixel values would be low in the initial phase. After the dye accumulates, the intensity values will increase. The dye will then be drained from the blood vessels. Hence, the intensity values will come back to their initial values. This is the reason to get the bell-shaped curve for abnormal people. But the area of the bell-shaped region varies according to the accumulation of dye in the blood vessels. The number of new blood vessels is directly proportional to the amount of dye accumulation. But if the curve is drawn for the normal person, almost a constant curve is obtained between intensity and time. This is because the dye accumulated in the new & abnormal blood vessel's capillaries causes a change in intensity in a CNV-affected FA. This type of accumulation does not occur in a normal person, and therefore, CNV is diagnosed with this property.

Hence, by studying the fluorescein dye pattern, the severity of CNV can be detected. The mean intensity values are calculated for the cropped regions of both normal and CNV affected regions, and the difference between them (A-B) is also calculated. This procedure is done repetitively for each image in the FA sequences. The curves are drawn from (A-B) and have been used to study the fluorescein dye pattern.

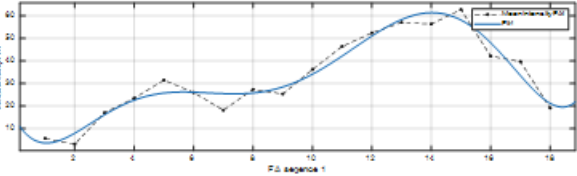
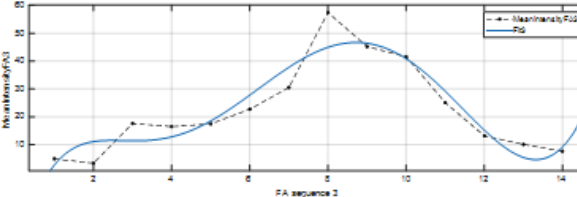
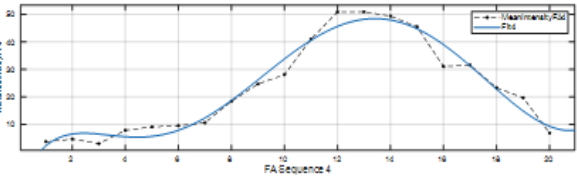
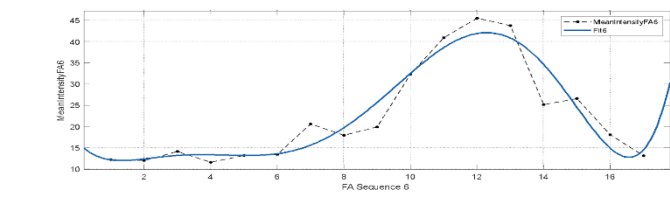
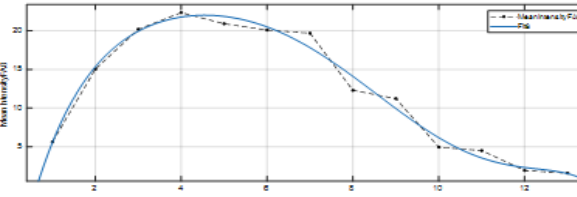
## 5 CURVE FITTING

The difference between the mean intensity values of normal and affected areas (A-B) is considered, and a graph is drawn with respect to time. A total of 50 sets of FA sequences are considered, and graphs are drawn for each set. Then a polynomial curve is drawn for the mean intensity values with respect to time using a curve-fitting technique. The coefficients are produced by the polynomial  $P(x)$  with a degree of 6, which is determined to be the best fit in terms of least squares. This polynomial is applied to the data (A-B) which is found to be nonlinear, and a polynomial of 6<sup>th</sup> order is chosen to be the best fit, which covers the nonlinearity compared to other polynomials. The 6th order polynomial generated for each FA sequence is shown for 5 people in Table 3, along with the actual curve and the approximated curve.

The generation of the curve is an interactive process. The curve interpolates and follows through with all the points of the data. The shape of the curve is adjusted by manipulating the control points, which guide segments of the curve as they are dragged through them. The newly obtained curve is known as the approximate curve. The equation represented by this curve can also be extracted. A 6th order polynomial curve has been determined to be the most suitable for the FA sequences used in this study. This polynomial curve is obtained for all the FA sequences, and four parameters are measured from the estimated curve.



TABLE.3 SIXTH ORDER POLYNOMIAL CURVES

Sl. No	<p style="text-align: center;"><b>Curve Fitting</b>  <b>6<sup>th</sup> order polynomial equation</b>  <math>f(x) = P1 * X^6 + P2 * X^5 + P3 * X^4 + P4 * X^3 + P5 * X^2 + P6 * X + P</math></p>
1.	 $f(x) = 0.0003403 x^6 - 0.019x^5 + 0.3934x^4 - 3.73 x^3 + 16.07x^2 - 23.12x + 14.05$
2.	 $f(x) = -0.0003769 x^6 + 0.02508x^5 - 0.5734x^4 + 5.77 x^3 - 26.48x^2 + 55.31x - 31.36$
3.	 $f(x) = -3.359e-05 x^6 + 0.003014x^5 - 0.0962x^4 + 1.343x^3 - 8.085x^2 - 20.54x - 11.55$
4.	 $f(x) = 0.0002802x^6 - 0.01312x^5 + 0.2217x^4 - 1.671x^3 + 5.882x^2 - 8.686x - 16.4$
5.	 $f(x) = -0.0002828 x^6 + 0.01213x^5 - 0.2028x^4 + 1.748 x^3 - 9.029x^2 + 27.34x - 14.33$

From the estimated 6<sup>th</sup> order polynomial curve, the parameters area under the curve, mean intensity at the early stage, mean intensity at the mid-stage, and mean intensity at the later stage are measured and tabulated for 10 patients, as shown in Table 4.

Table 4. Parameters estimated from the 6<sup>th</sup> order polynomial curve

FA sequence	Mean intensity at the early stage	Mean Intensity at the mid-stage	Mean Intensity at the late stage	Area under the curve (in pixels)	Grade
1	3.130	62.7108	29.4146	577.0965	Classic
2	4.517	117.777	25.2903	480.7766	Classic
3	3.321	57.4576	17.5236	306.9925	Occult
4	3.012	50.9984	21.5187	364.5429	Occult
5	3.739	46.5954	12.6893	348.8831	Occult
6	11.604	45.5207	18.0948	337.0114	Occult
7	3.894	46.4033	10.3761	335.5959	Occult
8	4.495	22.3381	15.0222	356.6657	Occult
9	6.071	101.705	26.346	483.453	Classic
10	5.671	100.994	27.374	320.966	Classic

## 6 IDENTIFICATION OF CNV USING MACHINE LEARNING CLASSIFIERS

A mathematical model is proposed using FA sequences that relies on the temporal variation of intensity. The features measured in the estimated model will efficiently help identify CNV. All of these extracted features are supplied to these classifiers: NN, SVM, DT, kNN, Ensemble, and NB classifiers. ML classifiers are effectively used for the categorization of biomedical images. The features extracted from the biomedical images, which are very helpful in making predictions or diagnoses of interest, are supplied to the ML classifier. Each classifier fits each data set differently. Therefore, the selection of an optimal classifier is crucial to achieving peak performance and accuracy.

The results of various classifiers compared with a deep neural network are shown in Table 5, and the performance indices are shown in Table 6. The results indicate that the NN, kNN, and DT classifiers deliver strong performance metrics in terms of accuracy, sensitivity, specificity, and F1 score. High F1 score of these classifiers indicates a good balance between precision and recall. It means the model has a low number of false positives and false negatives. The comparison of the performance indices such as Sensitivity, Specificity, Positive Predictive Value (PPV), Negative Predictive Value (NPV) and F1 score of these classifiers is given in Figure 3 and Figure 4.

TABLE 5. PERFORMANCE OF MACHINE LEARNING CLASSIFIERS ON FA DATA

Classifier	Accuracy (%)	Training time (Sec)
NN	98	0.0265
SVM	96	0.8885
DT	98	1.0234
kNN	98	1.1577
Ensemble	96	6.9185
NB	94	1.6586
DNN	98	9.8654(min)

TABLE 6. PERFORMANCE INDICES OF DIFFERENT CLASSIFIERS ON FA DATA

Classifier	Sensitivity (%)	Specificity (%)	PPV (%)	NPV (%)	F1 score
NN	96	100	100	96	98
SVM	92	100	100	92	96
DT	96	100	100	96	98
kNN	100	96	96	100	98
Ensemble	92	100	100	92	96
NB	92	96	96	92	94
DNN	100	96	96	100	98

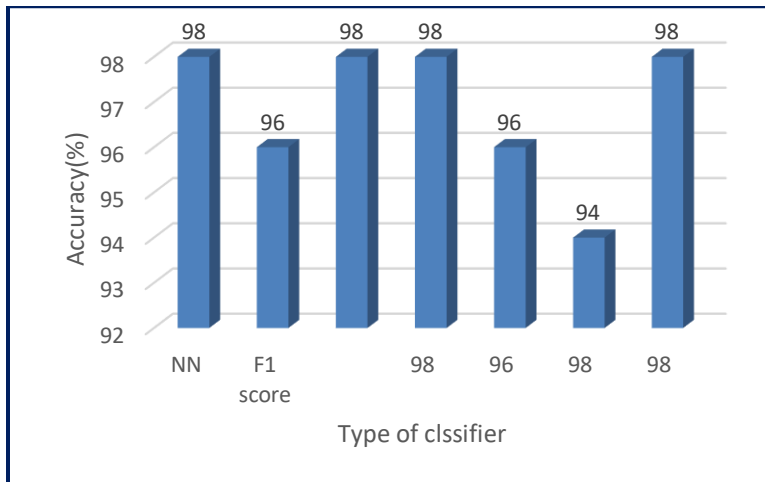


Figure 3. Detection of CNV through parametric modeling-Comparison of classifiers based on the accuracy

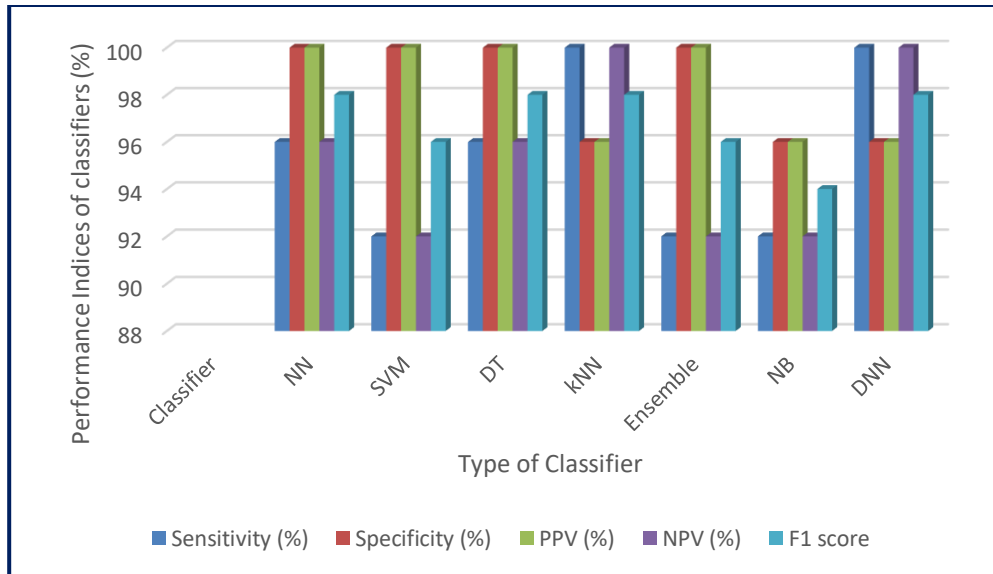


Figure 4. Detection of CNV through parametric modeling: Performance indices of classifiers

## 7. CONCLUSION

The FA images of the CNV patients were collected and pre-processed. The frames with appropriate light exposure were selected through histogram analysis. The ROI is cropped and the mean intensity values are measured for the normal and abnormal regions of each frame in FA sequences of 50 patients. A 6<sup>th</sup> order polynomial curve was drawn using a curve fitting technique and the salient parameters are extracted from the estimated curve. This proposed technique gives a feasible solution to detect the rise of abnormal vessels through the parameters extracted from the 6<sup>th</sup> order polynomial curve. Identifying the size and type of the lesion is essential for ophthalmologists to give proper treatment. Since the current techniques for evaluating CNV are based on qualitative assessment, this proposed quantitative assessment will help to analyze CNV automatically. It is also used to reduce inter- and intra-observer variability, which is a major problem in subjective evaluation. Features found in this model enhance the performance of all the classifiers. The NN, DT, and kNN classifiers achieve the same 98% accuracy as the DNN. Therefore, this mathematical model obviates the necessity of using a DNN in this case. The classification performance of all ML classifiers clearly shows that the accuracy obtained from each classifier is over 90%. Thus, the mathematically developed methods detect CNV effectively, irrespective of the type of classifiers.

### Acknowledgment

The authors gratefully acknowledge the Vasan Eye Care Hospitals, Chennai, for their contribution to data collection.

## REFERENCES

- [1] Grossniklaus, H. E., & Green, W. R. (2004). Choroidal neovascularization. *American journal of ophthalmology*, 137(3), 496-503.
- [2] Chamberlin, J. A., Bressler, N. M., Bressler, S. B., Elman, M. J., Murphy, R. P., Flood, T. P & Macular Photocoagulation Study Group, "The use of fundus photographs and fluorescein angiograms in the identification and treatment of choroidal neovascularization in the Macular Photocoagulation Study", *Ophthalmology*, 96(10), 1526-1534, 1989.
- [3] Berger JW, Yoken J. "Computer-assisted quantitation of choroidal neovascularization for clinical trials", *Invest Ophthalmol Vis Sci*,41(8):2286-95, 2000.
- [4] Shah, S.M., Tatlipinar, S., Quinlan, E., Sung, J.U., Tabandeh, H., Nguyen, Q.D., Fahmy, A.S., Zimmer-Galler, I., Symons, R.A., Cedarbaum, J.M. and Campochiaro, P.A, "Dynamic and quantitative analysis of choroidal neovascularization by fluorescein angiography", *Investigative ophthalmology & visual science*, 47(12), 5460-5468, 2006.
- [5] H. Narasimha-Iyer, A. Can, B. Roysam and J. Stern, "Automated Change Analysis From Fluorescein Angiograms for Monitoring Wet Macular Degeneration", *International Conference of the IEEE Engineering in Medicine and Biology Society*, New York, NY, pp. 4714-4717,2006.
- [6] E. Brankin, P. McCullagh, W. Patton, A. Muldrew and N. Black, "Identification of Choroidal Neovascularization on Fluorescein Angiograms Using Gradient Vector Flow Active Contours", "International Machine Vision and Image Processing Conference, Portrush, pp. 165-169,2008.
- [7] Ahmed S Fahmy, Walid M. Abdelmoula, Ahmed E. Mahfouz, Syed Mahmoud Shah, "Segmentation of Choroidal Neovascularization Lesions in Fluorescein Angiograms Using Parametric Modeling of the Intensity Variation", 978-1-4244-4128-0/11/\$25.00 ©2011 IEEE,2011.
- [8] Walid M. Abdelmoula, Syed M. Shah, Ahmed S. Fahmy, "Segmentation of Choroidal Neovascularization Fundus Fluorescein Angiograms", *IEEE Transactions on Biomedical Engineering*, VOL. 60, NO. 5, 2013
- [9] Lin, K. S., Tsai, C. L., Chen, S. J., & Lin, W. Y, "Automatic Evaluation of Choroidal Neovascularization in Fluorescein Angiography" *Advances in Intelligent Systems and Applications-Volume 2* (pp. 377-382). Springer, Berlin, Heidelberg, 2013
- [10] Chhablani, J., Deepa, M., Tyagi, M, "Fluorescein angiography and optical coherence tomography in myopic choroidal neovascularization", *Eye* 29, 519–524, 2015.
- [11] Khurana, R. N., Dupas, B., &Bressler, N. M. "Agreement of time-domain and spectral-domain optical coherence tomography with fluorescein leakage from choroidal neovascularization", *Ophthalmology*, 117(7), 1376-1380, 2010.
- [12] Mookiah, M. R. K., Acharya, U. R., Fujita, H., Koh, J. E., Tan, J. H., Noronha, K.,& Tong, L, "Local configuration pattern features for age-related macular degeneration characterization and classification", *Computers in biology and medicine*, 63, 208-218, 2015.
- [13] Potdar, K., &Kinnerkar, R, "A Comparative Study of Machine Learning Algorithms applied to Predictive Breast Cancer Data", *International Journal of Science and Research*, 5(9), 1550-1553, 2016.
- [14] Karankar, N., Shukla, P., & Agrawal, N, "Comparative study of various machine learning classifiers on medical data", *7th International Conference on Communication Systems and Network Technologies (CSNT)*, pp. 267-271, 2017.
- [15] Nabian, M, "A Comparative Study on Machine Learning Classification Models for Activity Recognition", *Journal of Information Technology & Software Engineering*, 7(04), 4-8, 2017.
- [16] Mohamed, A. E, "Comparative study of four supervised machine learning techniques for classification", *International Journal of Applied*, 7 (2), 2017.
- [17] Singh, J., Singh, G., & Singh, R, "Optimization of sentiment analysis using machine learning classifiers", *Human-centric Computing and Information Sciences*, 7 (1), 32, 2017.

- [18] Sotiropoulos, D. N., Pournarakis, D. E., & Giaglis, G. M, “SVM-based sentiment classification: A comparative study against state-of-the-art classifiers”, *International Journal of Computational Intelligence Studies*, 6(1), 52-67, 2017.
- [19] Sonar, P., Bhosle, U., & Choudhury, C, “Comparative study of different machine learning classifiers for mammograms and brain MRI images”, *International Journal of Image Mining*, 3(2), 152-174, 2018.
- [20] Galveia, J. N., Travassos, A., Quadros, F. A., & da Silva Cruz, L. A, “Computer aided diagnosis in ophthalmology: Deep learning applications”, *Classification in BioApps* (pp. 263-293). Springer, Cham, 2018.
- [21] Jin, K., Yan, Y., Chen, M., Wang, J., Pan, X., Liu, X., ... & Ye, J. (2022). Multimodal deep learning with feature level fusion for identification of choroidal neovascularization activity in age-related macular degeneration. *Acta Ophthalmologica*, 100(2), e512-e520.
- [22] Wang, J., Hormel, T. T., Tsuboi, K., Wang, X., Ding, X., Peng, X., ... & Jia, Y. (2023). Deep learning for diagnosing and segmenting choroidal neovascularization in OCT angiography in a large real-world data set. *Translational Vision Science & Technology*, 12(4), 15-15.



**Dr. G. Anitha** completed her B.E. at the Government College of Technology, Coimbatore, her M.E. at the Madras Institute of Technology, Anna University, and her Ph.D. at the B.S. Abdur Rahman Institute of Science and Technology, Chennai. Her areas of interest include image and signal processing, machine learning, and deep learning. She has 16 years of teaching experience and 10 years of research experience, with 15 research articles published in reputable international journals and conferences. Currently, she is an Assistant Professor in the Department of Electronics and Instrumentation Engineering at B.S. Abdur Rahman Crescent Institute of Science & Technology, Chennai, India. You can reach her at [anidhag@crecent.education](mailto:anidhag@crecent.education)



**Dr. M. Mohamed Ismail** received B.E degree from Madurai Kamaraj University and M.S degree from BITS, Pilani and the Ph.D degree from JNTU, Hyderabad. His interested area of research is VLSI, Microprocessor, Embedded systems and wireless sensor networks. He has got 30 years of teaching and research experience. Published more than 30 research articles in the reputed International journals and Conferences. So far two scholars have completed Ph.D degree and five more research scholars are working under his supervision. He is currently working as Professor in the Department of Electronics and Communication Engineering, B.S. Abdur Rahman Crescent Institute of science & Technology, Chennai, India. Email id: [mmismail@crecent.education](mailto:mmismail@crecent.education)